Chapter 11
The Peculiarities of Nanostructures Formation in Liquid Phase

An.D. Zolotarenko, Al.D. Zolotarenko, E. Rudakova, S.Yu. Zaginaichenko, A.G. Dubovoy, D.V. Schur, V.A. Lavrenko, A.E. Perekos, V.P. Zalutskiy, M.M. Divizinyuk, E.V. Azarenko, and Yu.A. Tarasenko

Abstract The processes occurring on the electrodes and in the liquid phase during the arc discharge in the liquid phase (ADLP) have been considered in the present work and we explain the mechanism of carbon nanostructures (CNS) formation proposing the model based on the analysis of existing regularities in behaviour of charged particles under extreme temperature and pressure gradients.

The CNS synthesis by ADLP method has been performed in dielectric liquids: hydrocarbons, liquid gases (N_2, Ar, He, etc.), deionized water and others. Suspension containing clusters of synthesized nanostructures has been formed by the synthesis.

The efficiency of this method is sharply increased by using arc discharge in the liquid phase where powder reagent layer is used as anode. To increase the frequency of electrodes clamping and moving apart, an electromagnetic vibrator has been used in this method and it brings and takes away the cathode from the powder reagent at a specified frequency. For ADLP, nanostructures form simultaneously at several points on the conducting particle surface as a result of microscopic acts of arc discharge.

An.D. Zolotarenko (✉), Al.D. Zolotarenko, E. Rudakova, S.Yu. Zaginaichenko, A.G. Dubovoy, D.V. Schur, and V.A. Lavrenko
Institute for Problems of Materials Science of NAS of Ukraine,
Krzhyzhanovsky str. 3, Kiev 03142, Ukraine
e-mail: a.d.zolotarenko@gmail.com

A.E. Perekos and V.P. Zalutskiy
Institute for Metal Physics of NAS of Ukraine, 36 Acad., Vernadsky Boulevard,
UA-03680, Kiev-142, Ukraine
e-mail: perekos@ukr.net

M.M. Divizinyuk and E.V. Azarenko
Sevastopol National University of Nuclear Energy and Industry, Kurchatov str. 7,
Sevastopol 99033, Ukraine
e-mail: shumira_07@mail.ru

Yu.A. Tarasenko
O. Chuiko Institute of Surface Chemistry of NAS of Ukraine,
17 General Naumov street, Kiev 03164, Ukraine
e-mail: nikar@kartel.kiev.ua

S.Yu. Zaginaichenko et al. (eds.), *Carbon Nanomaterials in Clean Energy Hydrogen Systems - II*, NATO Science for Peace and Security Series C: Environmental Security 2,
DOI 10.1007/978-94-007-0899-0_11,

These nanostructures are generated from the liquid phase and anode vapors and represent the product exhibiting rather interesting physical and chemical properties.

Based on the analysis of the observations performed in the course of carbon nanostructures synthesis, the model of nanostructures formation by arc discharge in the liquid phase has been proposed in this paper. Presence and absence of deposit on the cathode have been explained.

Keywords Me-C nanocomposite · Structure · Phase composition · Arc discharge · Liquid phase · Specific magnetization

11.1 Introduction

Materials which physical properties can be controlled by varying them within wide limits occupy a particular place among modern metallic materials. These materials are used extensively in different fields of engineering and industry and define to a large extent the pace of scientific and technical progress. Magnetic metals and alloys can be realistically assigned to such materials [1, 2].

Magnetic properties of metals and alloys depend on many technological and physical factors: conditions of their production, chemical composition, structural state, number and distribution of different stable and metastable phases in a material, etc. which in turn are determined to a large measure by different types of external actions on a material during its production (mechanical, thermal, magnetic, thermo-mechanical, thermomagnetic, ultrasonic, etc. treatments) [3].

Synthesis of superfine, ultradispersed and nanodispersed magnetic materials provides unique possibilities for physicists and technologists. Magnetic properties of materials with the superfine or ultradispersed structure can be changed over very a wide limits by varying their dispersion, phase state, surface state and other factors [4, 5]. This paper realizes one of such possibilities by the example of superfine iron and nickel powders produced by the method of electric arc dispersion in dielectric liquid media (DDLM).

After the discovery of fullerenes and carbon nanotubes methods of their synthesis has been constantly investigated and improved. In parallel with the arc method in the gaseous phase and the pyrolytic method of synthesis of carbon nanostructures, since 2000 we have investigated and developed the method of arc synthesis in the liquid phase (ASLP). For the last decade, this method is used in increasing frequency to produce different nanostructures as the method alternative to the arc discharge in the gaseous phase (ADGP).

In the eighties we began our work on producing ultradispersed metal powders by the electroerosion method [6–8] and continue it today. Besides carbon nanostructures produced by evaporation of carbon electrodes in the liquid phase, there appears a possibility to produce metal-carbon composites by sublimation of metal in the carbon-containing liquid. In this case the metal nanoparticles form along with carbon nanostructures on their surface.

The main positive features [5, 8] of the method used are as follows:

1. high temperature in the arc zone, >4,000 K;
2. high cooling rate of evaporated products, $>10^9$ K/s;
3. high degree of dispersion. The particles range in size from 1 to 100 nm;
4. high nucleation rate at a low growth rate of a particle.

This method does not require using of unhealthy gases, vacuum equipment or expensive lasers. The proposed method provides a possibility of producing a wide range of materials by varying the conditions for synthesis and it presents a way of modifying the chemical composition of electrodes and a medium, in which the synthesis is carried out [9]. At present time different research groups over the world are engaged in such studies [10–19]. The liquid phase may be of different chemical compositions that affect the structure and composition of the produced nanoobjects being studied (Fig. 11.1).

In the present work we have considered the processes occurring on the electrodes and in the liquid phase during the arc discharge in the liquid phase process and explained the mechanism of carbon nanostructures (CNS) formation proposing the model based on the analysis of existing regularities in behaviour of charged particles under extreme temperature and pressure gradients.

The Me-C composites have been produced by the arc discharge method in toluene using a powder metal anode (ADIP); their structure, phase composition and magnetic properties have been studied.

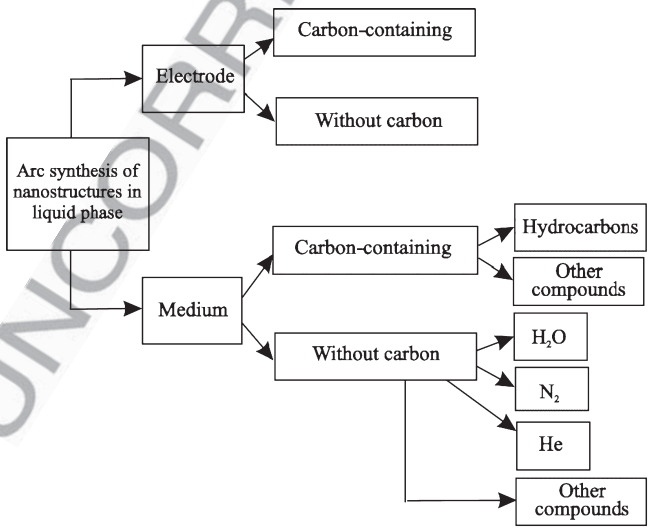

Fig. 11.1 Diagram for possible combinations of medium and electrode materials in synthesis of nanostructures by the arc method in the liquid phase

11.2 Experimental

Synthesis of nanoparticles in the liquid phase has been carried out in the installation specially designed for these studies (Fig. 11.2). This installation allows the metal and graphite electrodes to be evaporated by an electric arc in the liquid medium in the temperature range from 4 to 340 K. In the neighbourhood of the cathode the arc temperature may be as much as $1{,}2 \cdot 10^4$ K at currents of 200–300A (Fig. 11.3).

The electronic control block is simple to operate and provides a possibility of varying and measuring voltage and electric current. These changes make it possible

Fig. 11.2 The installation for synthesis of nanocarbon structures and Me-carbon composites in the liquid phase

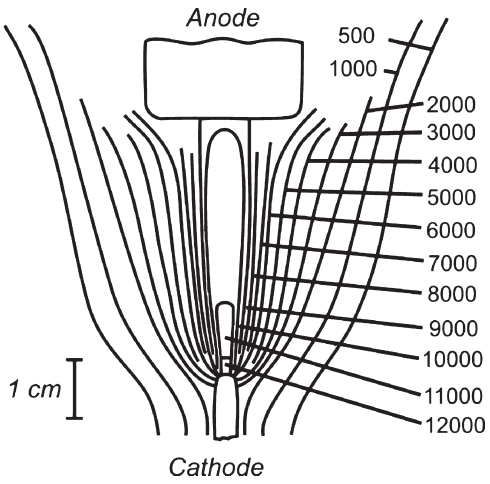

Fig. 11.3 Temperature distribution (in K) in different regions of the electric arc between the carbon electrodes at strength of current equal to 200A [19]

to affect the conditions of the plasmochemical process in the reactor and the product morphology and yield.

All the chemical reagents used in the synthesis have been subjected to the prior purification and rectification. Type MPG-7 graphite has been used. The graphite rods have been pre-annealed in vacuum. The metallic rods have been remelted repeatedly in an arc furnace in the spectro-pure argon medium.

Crystalline structures and phase compositions of powders have been determined using X-ray diffractometer DRON-3.0 in Cok_α irradiation; magnetic properties have been measured on a ballistic magnetometer; dimensions of the coherent-scattering region (CSR) have been calculated by X-ray lines broadening with Selyakov-Sherrer formula.

11.3 Results and Discussion

Table 11.1 represents the results of studies on initial iron and nickel powders and the product prepared by arc discharge in the liquid phase using a powder anode (ADIP) in toluene. Also, this table gives the data on Fe(B-5-2) and Ni(B-2) powders before and after thermo-magnetic measurements. Figures 11.4–11.9 and Table 11.2 illustrate the results of measurements of magnetic properties: specific saturation magnetization, σ_s, coercive force, H, and residual induction, I_R; in this case Figs. 11.4–11.7 demonstrate field dependences of specific magnetization and Figs. 11.8–11.9 show temperature dependences.

Diffraction patterns of initial iron and nickel powders show only lines of *bcc* iron and *fcc* nickel, respectively. After ADIP treatment in toluene, the phase composition of synthesized powders has changed. The diffraction pattern of Fe (B-5-2) powder demonstrates two crystalline phases, α-Fe (~24%) and Fe_3C (~76%). In addition to the lines for pure nickel, the diffraction pattern of Ni(B-2) powder has the most intensive line for carbon solid solution in nickel. In magnetic

Table 11.1 Phase composition and dimension of CSR for iron and nickel powders

Sample	Phase composition	Content, %	D, nm
Fe powder, initial state	α- Fe	100	270
	α- Fe	24	–
Fe powder (B-5-2)	Fe_3C	76	24
Ni powder, initial state	Ni	100	150
	Ni	96	
Ni powder (B-2)	Ni-C	4	150
	α-Fe		
	Fe_3C	73	110
	Fe_3O_4	11	40
Fe powder (B-5-2), after heating	FeO	16	100
Ni powder (B-2), after heating	Ni	100	130

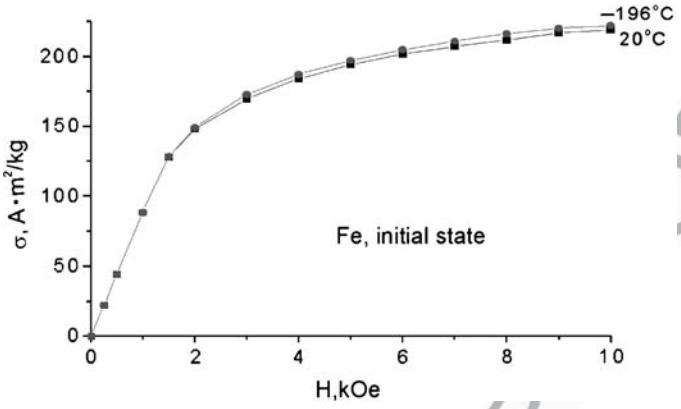

Fig. 11.4 Field dependence of specific magnetization of initial iron powder at temperatures T = −196°C and 20°C

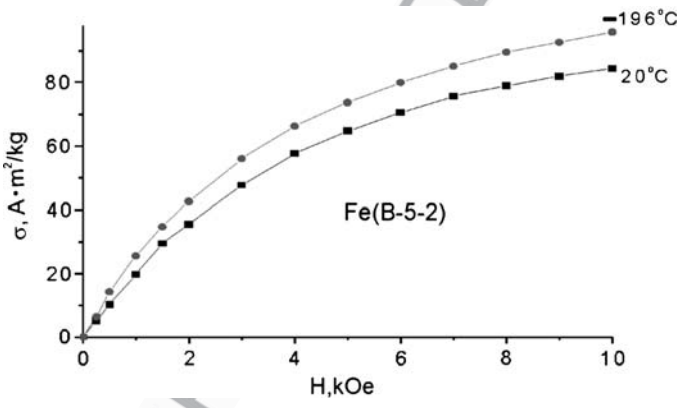

Fig. 11.5 Field dependence of specific magnetization of Fe-C nanocomposite at temperatures T = −196°C and 20°C

thermograms, Curie temperatures 400 and 760°C for iron powders (Fig. 11.8) and 225 and 360 C for nickel powder (Fig. 11.9) correspond to these phases. For Me-C composites, specific saturation magnetization of nickel powder is almost unchanged (Figs. 11.6 and 11.7, Table 11.2); this is related to a low amount of Ni-C crystalline phase that is formed in powder by ADIP treatment. Specific saturation magnetization of Fe-C composites changes more significantly (Figs. 11.4 and 11.5, Table 11.2). This is conditioned by the considerable change in the phase composition of iron powders after ADIP treatment. In the course of synthesis, initial α-Fe transforms into carbide Fe_3C almost completely (Table 11.1). For the products, changes in coercive force, H, and residual induction, I_R, are attributable to the corresponding changes in the phase composition and dispersivity of the powders.

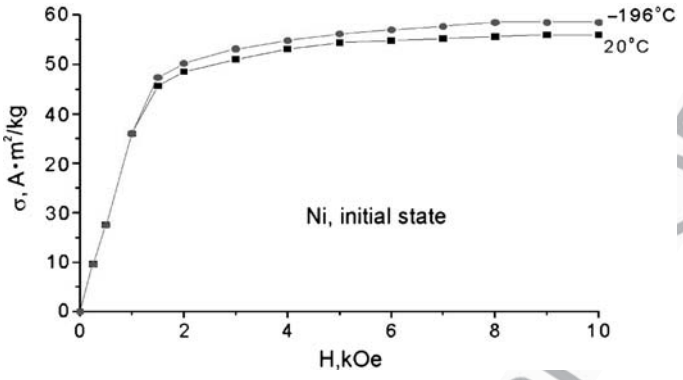

Fig. 11.6 Field dependence of specific magnetization of initial nickel powder at temperatures T = −196°C and 20°C

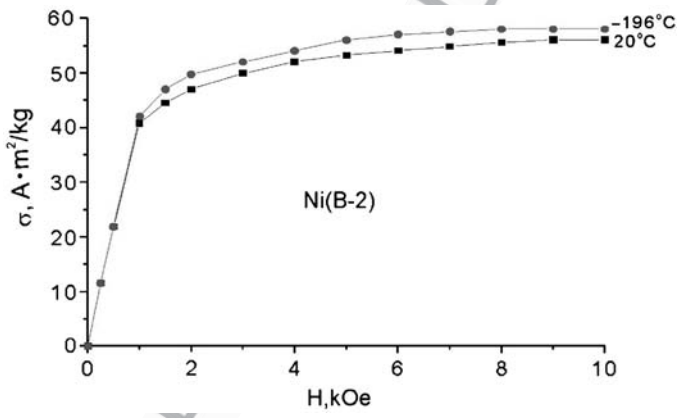

Fig. 11.7 Field dependence of specific magnetization of Ni-C nanocomposite at temperatures T = −196°C and 20°C

The results of the change in the powders phase composition after heating in measuring the temperature dependence of specific saturation magnetization are also of interest. As can be seen from Figs. 11.8, 11.9 and Table 11.1, the phase compositions of iron and nickel in the synthesized powders are changed significantly on heating. After heating, the line of Ni-C solid solution has disappeared from the diffraction pattern of Ni(B-2) powder. After heating in the diffraction pattern of Fe(B-5-2) powder intensities of the lines of Fe_3C carbide have reduced, intensities of lines of α-Fe increased and the lines of crystalline phases FeO and Fe_3O_4 appeared. After heating and on subsequent cooling the knee at ~225°C (Ni-C solid solution) has disappeared from the magnetic thermogram of Ni(B-2) powder. On further cooling, in addition to the knees at ~760°C (α-Fe) and ~400°C

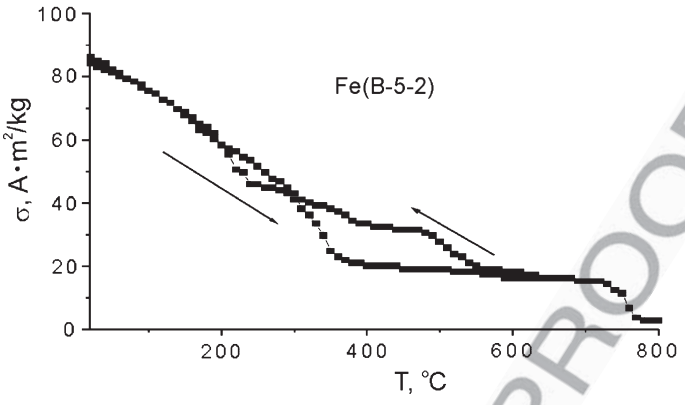

Fig. 11.8 Temperature dependence of specific magnetization of Fe-C nanocomposite before and after heating to 800°C

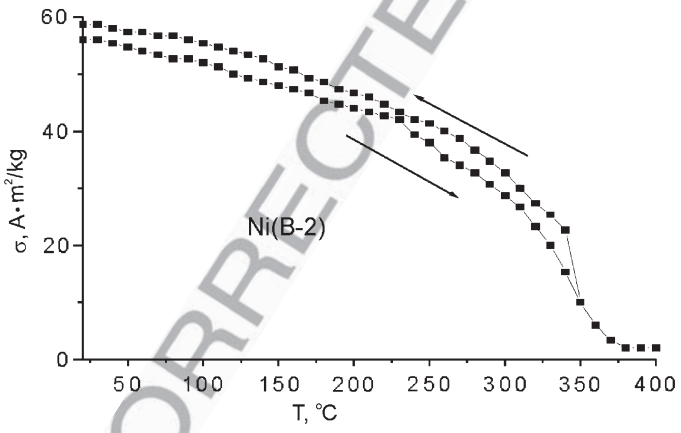

Fig. 11.9 Temperature dependence of specific magnetization of Ni-C nanocomposite before and after heating to 400°C

t2.1 **Table 11.2** Magnetic properties of iron and nickel powders

		σ_s, A·m²/kg			
t2.3	Material	20°C	−196°C	H, Oe	I_R, Gs
t2.4	Ni, initial	56	58.5	50	1,434
t2.5	Fe, initial	219	222	6	102.2
t2.6	Ni(B-2)	56	58	50	860
t2.7	Fe(B-5-2)	84.3	95.8	20	108.7

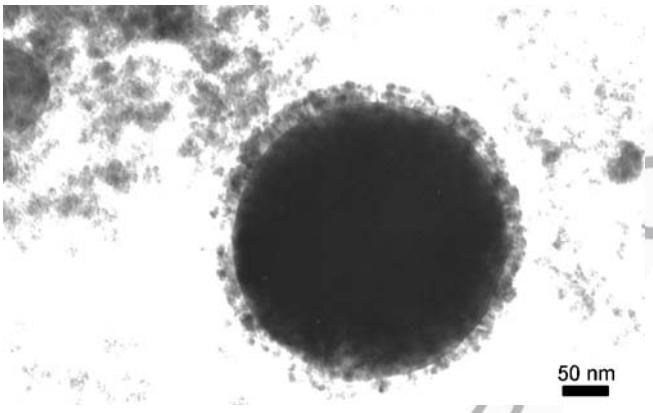

Fig. 11.10 TEM photograph of Ni microgranule (250 nm) in nanocarbon shell

(Fe_3C), the knee at ~600°C corresponding to the Curie temperature for Fe_3O_4 oxide has also appeared in the thermogram of Fe(B-5-2) powder.

On the basis of TEM observations, one can note that the synthesized nanocomposites of both iron and nickel contain particles 1–400 nm in diameter. The most part of particles have a diameter ranging from 10 to 20 nm (Figs. 11.10 and 11.11).

The shell on the large nickel particles (Fig. 11.10) indicates that this particle is formed from the melt. Interaction of melted Ni and carbon vapor gives rise to Ni_3C carbide that decomposes during the alloy crystallization with liberation of carbon. The carbon forms graphite-like nanostructures on the particle surface.

Large iron particles (~150 nm) do not have such prominent boundaries, although all particles of 10–30 nm fractions are enclosed in the carbon shells.

In addition, iron nanoparticles formed by the arc magnetic field exhibit residual magnetization. This causes the nanoparticles to agglomerate in spherical clusters up to 1 μm in diameter (Fig. 11.12).

11.4 Model of Process

The CNS synthesis by the ADLP method has been performed in dielectric liquids: hydrocarbons, liquid gases (N_2, Ar, He, etc.), deionized water and others. Suspension containing clusters of synthesized nanostructures has been formed by the synthesis.

Discharge in liquid is initiated by moving apart electrodes that were initially clamped. The high-temperature arc column that appears between the electrodes converts both the anode material and the liquid phase surrounding this anode into the vapor phase. In the case that electrode spacing does not exceed 1 mm, the deposit similar to that formed in ADGP has been generated on the cathode. Deposit

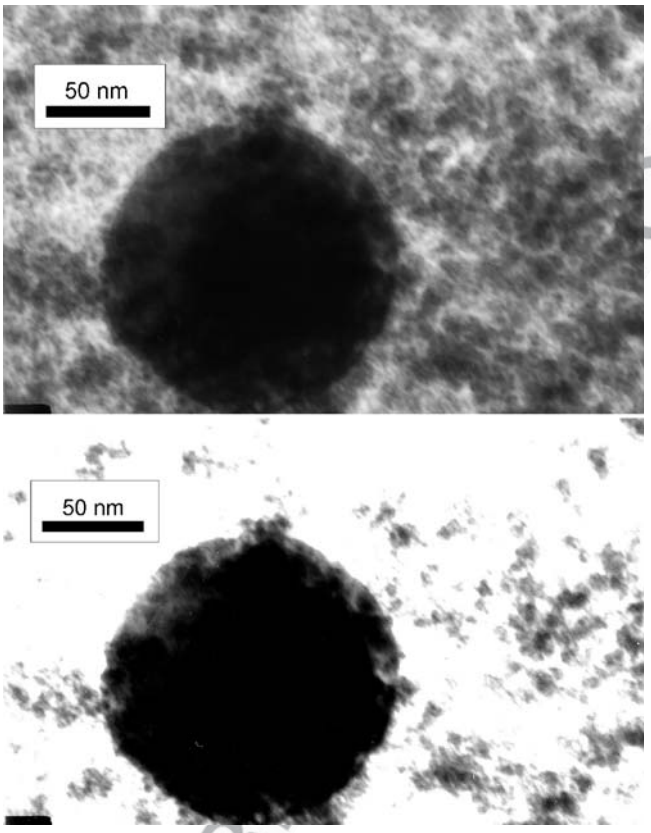

Fig. 11.11 TEM photographs of Ni microgranule (100 nm) in nanocarbon shell

on the cathode is not formed as the electrodes moving apart is more than 1 mm. In this situation the whole resulting product is either in suspension in the liquid phase or on the bottom as sediment.

The efficiency of this method is sharply increased by using the arc discharge in the liquid phase where a layer of powder reagent is used as an anode (Fig. 11.13). In this case in displacement of electrodes, each conducting particle being among the similar ones is, on the one hand, an anode and, on the other hand, a cathode. To increase the frequency of electrodes moving together and apart, an electromagnetic vibrator has been used in this method and it brings and takes away the cathode from the powder reagent at a specified frequency. A large amount of nanoproduct has been formed as a result of great number of electric discharges.

On the basis of our phenomenological model of processes occurring in the interelectrode space in the liquid phase, the following variants of the process course can be assumed.

1. During ADLP, when the electrode separation is less than 1 mm, liquid phase transformed into a vapor state (Fig. 11.14), thus providing conditions similar to

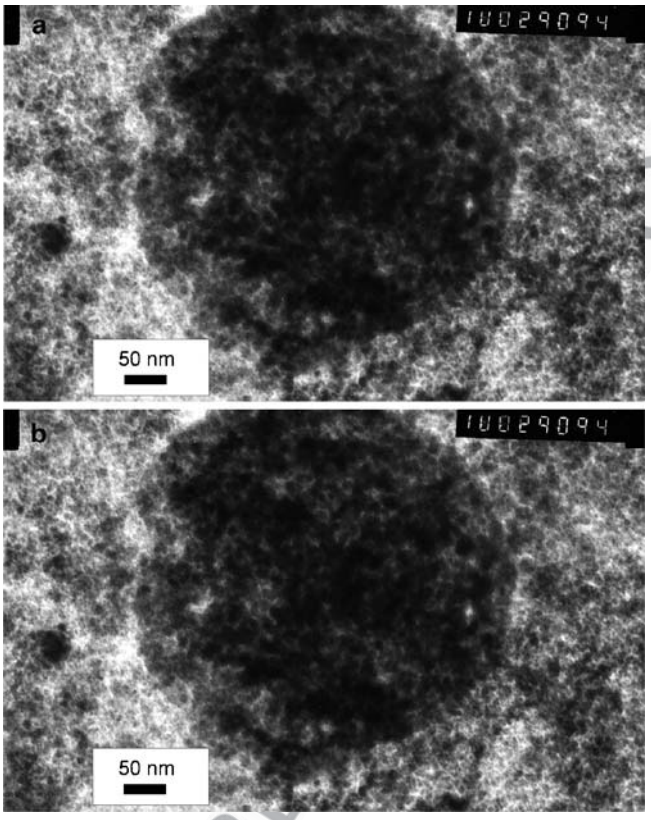

Fig. 11.12 Spherical clusters consisting from ferromagnetic nanoparticles

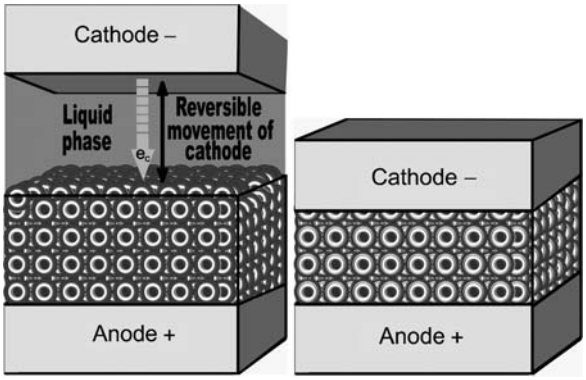

Fig. 11.13 Schematic diagram of operation of the arc discharge unit in the liquid phase with a dispersed anode

those in ADGP. As this takes place, carbon vapor, carbon nanostructures and fragments of graphene sheets interact with each other under the action of electromagnetic forces and move in different directions.

At the interface (g-*l*) the vapor phase condenses due to the temperature gradient. The charged particles, moving from the anode to the cathode, form the deposit. A minor amounts of these particles, by virtue of collision with an electron stream, in concert with neutral particles are ejected from the arc zone and quenched in crossing the interface.

Near the quenching zone, the particles comprising the gaseous phase agglomerate through the saturation of nonsaturated bonds, create different nanoforms and assemble in clusters.

2. When electrodes are moved apart at the distance exceeding a vapor bubble diameter, the deposit formation will stop on the cathode (Fig. 11.14b). This can be derived from the fact that the particles, forming the deposit and having plasma temperatures, are bound now to overcome the layer of liquid to reach the cathode. Approaching to the interface (g-*l*), these particles undergo the quenching process. In the quenching zone, the particles begin to agglomerate, form clusters and lose completely their reactivity.

Breaking away from the anode surface, the bubbles go into the volume of liquid phase (Fig. 11.14c). All structures contained in a bubble and formed as a result of the anode evaporation remain the volume-enclosed of the bubble.

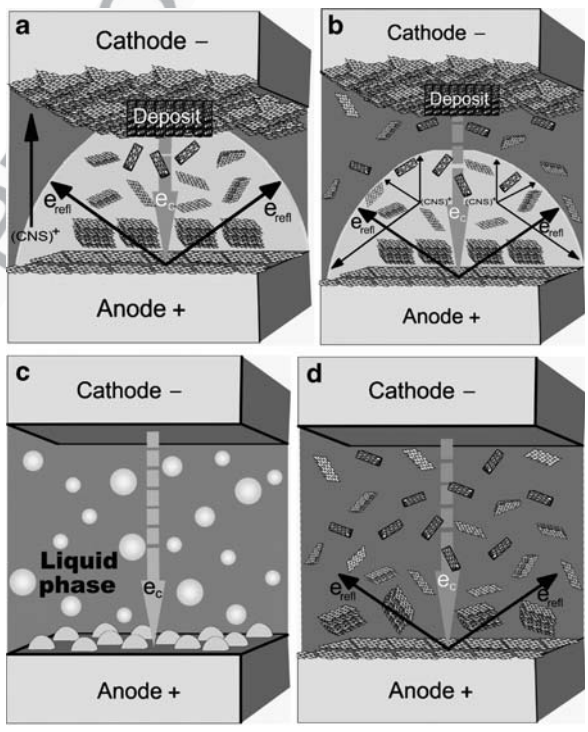

Fig. 11.14 The mechanism of formation of carbon nanostructures and their composites in the liquid phase

Vapor, getting to the zone of lower temperatures, condenses, the bubbles are shuted and their content turn into the liquid phase (Fig. 11.14d). In the liquid nanoparticles can assemble in clusters and precipitate or can be in suspension.

In the case of co-evaporation of metal and graphite or metal in the hydrocarbons medium, the metallic nanoparticles encapsulated in the carbon matrix or other composites can be produced by condensation of vapours mixture in the shutting bubbles.

3. In the case that powder reagent layer is used as an anode, the nanostructures form simultaneously at several points on the surface of current-conducting particle as a result of microscopic acts of arc discharge, similarly as shown in Fig. 11.14a. These nanostructures are generated from the vapours of liquid phase and anode and represent the product exhibitied rather interesting physical and chemical properties.

11.5 Conclusions

In the present work Me-C nanocomposites have been produced by the ADIP method. Their structure, phase composition and magnetic properties have been studied.

The performed studies have shown that Me-C composites have a significantly changed phase composition. The α-Fe powder transforms into Fe_3C carbide almost completely and solid carbon solution in nickel (Ni-C) forms in the Ni powder.

Heating the synthesized nanocomposites also leads to the change in their phase composition: after heating, a crystalline phase Ni-C disappears in the Ni(B-2) powder, and oxides (FeO and Fe_3O_4) appear in the powder Fe(B-5-2) as well as the ratio of crystalline phases (α-Fe and Fe_3C) changes.

Based on the analysis of the observations performed in the course of carbon nanostructures synthesis, the model of nanostructures formation by arc discharge in the liquid phase has been proposed in this paper.

The presence and absence of deposit on the cathode have been explained in consequence of the experiments performance.

Acknowledgment The work has been done within the framework of STCU project 4919.

References

1. Vonsovskiy SV (1971) Magnetism. Nauka, Moscow, p 1032 (in Russian)
2. Vonsovskiy SV (ed) (1961) Magnetic properties of metals and alloys. Gostekhizdat, Moscow, p 560 (in Russian)
3. Gusev AI, Rempel AA (2004) Nanocrystalline materials. Cambridge International Science, Cambridge, p 149

4. Chuistov KV, Shpak AP, Perekos AE et al (2003) Small-size metallic particles: production conditions, atomic and electron structure, magnetic properties and practical implementation. Usp Fiz Met 4(4):235–245
5. Chuistov KV, Perekos AE, Zalutskiy VP et al (1997) The effect of production conditions on structural state, phase composition and fineness of iron and iron-based powders made by electric-spark erosion. Met Phys Adv Technol 16(8):865–875
6. Dubovoy AG, Perekos AE, Chuistov KV (1985) Structure and magnetic properties of small amorphous particles of metallic Fe-15 at.% B alloy. Phys Met 6(5):1085–1088
7. Dubovoy AG, Zalutskiy VP, Ignat'ev IYu (1990) Structure, magnetic parameters and thermal stability for small amorphous particles and amorphous strips of Fe-15 at.% B. Phys Met 8 (4):804–807
8. Chuistov KV, Perekos AE (1998) Structure and properties of small-size metallic particles. 1. Phase-structure state and magnetic characteristics (Review). Met Phys Adv Technol 17 (1):57–84
9. Schur DV, Dubovoy AG, Zaginaichenko SYu, Adejev VM, Kotko AV, Bogolepov VA, Savenko AF, Zolotarenko AD (2007) Production of carbon nanostructures by arc synthesis in the liquid phase. Carbon 45(6):1322–1329
10. Loiseau A, Demoncy N, Stephan O et al (2000) Filling carbon nanotubes using an ARC discharge, Science and application of nanotubes. Kluwer Academic Publishers, New York, p 398
11. Schur DV, Dubovoy AG, Lysenko EA et al (2003) Synthesis of nanotubes in the liquid phase. In: Extended abstracts of 8th international conference on hydrogen materials science and chemistry of carbon nanomaterials (ICHMS'2003), Sudak (Crimea, Ukraine), p 399–402
12. Schur DV, Dubovoy AG, Zaginaichenko SYu, Savenko AF (2004) Method for synthesis of carbon nanotubes in the liquid phase.In: Extended abstracts of international conference on carbon, providence (Rhode Island, USA). American Carbon Society p 196–198
13. Antisari MV, Marazzi R, Krsmanovic R (2003) Synthesis of multiwall carbon nanotubes by electric arc discharge in liquid environments. Carbon 41(12):2393–2401
14. Biro LP, Horvath ZE, Szalmas L et al (2003) Continuous carbon nanotube production in underwater AC electric arc. Chem Phys Lett 372(3–4):399–402
15. Sano N, Nakano J, Kanki T (2004) Synthesis of single-walled carbon nanotubes with nanohorns by arc in liquid nitrogen. Carbon 42(3):686–688
16. Qui J, Li Y, Wang Yu et al (2004) Synthesis of carbon-encapsulated nickel nanocrystals by arc-discharge of coal-based carbons in water. Fuel 83(4–5):615–617
17. Bera D, Kuiry SC, McCutchen M et al (2004) In-situ synthesis of palladium nanoparticles-filled carbon nanotubes using arc discharge in solution. Chem Phys Lett 386(4–6):364–368
18. Montoro LA, Lobrano Renata CZ, Rosolen JM (2005) Synthesis of single-walled and multi-walled carbon nanotubes by arc-water method. Carbon 43(1):200–203
19. Ishlinsky AYu (1989) Polytechnic dictionary. Soviet Encyclopedia, Moscow, p 611 (in Russian)